The Wigner - Seitz model for concentrated clay suspensions

1997 J. Phys.: Condens. Matter 9 2683

(http://iopscience.iop.org/0953-8984/9/13/005)

J. Phys.: Condens. Matter **9** (1997) 2683–2692. Printed in the UK PII: S0953-8984(97)78742-3

The Wigner–Seitz model for concentrated clay suspensions

Emmanuel Trizac† and Jean-Pierre Hansen‡

Laboratoire de Physique (URA 1325 du CNRS), Ecole Normale Supérieure de Lyon, 69364 Lyon Cédex 07, France

Received 17 October 1996

Abstract. The model of a single uniformly charged finite platelet confined with its counter-ions and added salt to a Wigner–Seitz cell is treated within linearized Poisson–Boltzmann (or Debye–Hückel) theory. We consider circular (disc-like) and square platelets placed at the centre of a cylindrical or parallelepipedic cell of volume fixed by the macroscopic clay concentration. For a given volume the free energy F is minimized with respect to the aspect ratio of the cell. We find that the quadrupole moment Q of the total charge distribution always vanishes at the free-energy minimum, and that for discs, Q and F are practically identical for the two cell geometries at any given volume and salt concentration. Finally we propose a hybrid Poisson–Boltzmann/Debye–Hückel formulation which allows non-linearities to be approximately accounted for.

1. Introduction

Clay colloid suspensions consist of thin crystalline silicate platelets carrying structural surface charges, dispersed in water, in the presence of counter-ions and salt. The platelets are typically 1 nm thick, irregularly shaped with lateral dimensions of a few tens or hundreds of nm, and the surface charge density is typically an elementary charge $(-e)$ per nm^2 [1]. Although large natural clay platelets are somewhat flexible, smaller synthetic clay platelets, like disc-shaped laponite [2], can be regarded as rigid.

A statistical description of concentrated dispersions, even of monodisperse and single-shaped platelets, is very difficult, because of the considerable anisotropy of the interacting double layers around each clay particle [3]. In two recent articles [4, 5], we considered the problem of a single clay platelet confined to a Wigner–Seitz (WS) cell together with co- and counter-ions, such that the total charge of the cell is zero. The shape of the WS cell supposedly reflects the mean shape of the 'cage' formed by neighbouring platelets. Although the concept of a WS cell is well defined only in the case of a regular lattice, it has been widely used in the description of the local structure in liquids [6] and suspensions. For spherical colloidal particles, the obvious shape of the WS cell is a concentric sphere [7], but for anisotropic particles like rods [8] or platelets, the shape of the WS cell and that of the particles match only when the latter are aligned. In reference [4], we considered a circular platelet in a spherical WS cell appropriate for dilute suspensions where the platelets may rotate freely, and in a co-axial cylindrical WS cell which is better adapted to concentrated suspensions or swollen clays where particles are stacked in parallel arrays.

In this paper, we consider both disc-shaped and square platelets in parallelepipedic WS cells. For any given concentration of platelets (which determines the volume of the WS

† e-mail: etrizac@physique.ens-lyon.fr.
‡ e-mail: hansen@physique.ens-lyon.fr.

0953-8984/97/132683+10$19.50

cell) and of salt, the optimum aspect ratio of the cell is determined by minimizing the free energy calculated within the linearized Poisson–Boltzmann approximation. We also investigate the variation of the total quadrupole moment of the cell with the aspect ratio. The results for disc-like platelets are compared to our earlier results for a cylindrical WS cell. Finally, within the latter geometry, we introduce a hybrid Poisson–Boltzmann/Debye–Hückel formulation, allowing an improvement over the fully linearized theory which is known to be inadequate for highly charged platelets. This formulation can be regarded as an extension of the classic Gouy–Chapman theory [11] for infinite charged planes to finite-size platelets, which takes into account edge effects.

2. Poisson–Boltzmann theory in a Wigner–Seitz cell

Consider a single, infinitely thin clay platelet $\mathcal{P}$, carrying Z elementary charges $-e$ assumed to be uniformly distributed over a surface S, placed at the centre of a WS cell of prescribed topology and of volume $V = 1/n$, where n is the clay concentration (number of platelets per unit volume). The platelet is suspended with its monovalent (positive) counter-ions in a 1:1 salt solution; the solvent (water) is assumed to be a continuum of dielectric constant ε. Depending on the situation under scrutiny, various boundary conditions can be applied on the surface Σ of the WS cell corresponding to various local environments of the clay platelet [4]. We will consider the cases where the WS cell is associated with a crystalline array of clay particles or where the average topology of the cage formed by neighbouring platelets can be approximated in such a way. The normal component of the electric field therefore vanishes everywhere on the surface Σ. In the following, we shall address the cases of disc-shaped platelets in cylindrical or parallelepipedic cells (section 3), and of square platelets in parallelepipedic cells (section 4).

In Poisson–Boltzmann (PB) theory, the micro-ions are considered as an inhomogeneous ideal gas: the local densities of co- and counter-ions are then related to the electrostatic potential $\varphi(\boldsymbol{r})$ by

$$\rho^{\pm}(\boldsymbol{r}) = \rho_0^{\pm} \exp\left[\mp\beta e\varphi(\boldsymbol{r})\right] \tag{1}$$

where $\beta = 1/(kT)$.

The Debye–Hückel (or linearized Poisson–Boltzmann) approximation consists in linearizing the relation between the densities and φ around $\varphi(\boldsymbol{r}) = \varphi^{\star}$. This can be done by specifying $\boldsymbol{r}_0$ where $\varphi^{\star} = \varphi(\boldsymbol{r}_0)$. Alternatively, a simple choice consists in taking $\varphi^{\star} = \overline{\varphi}$ where $\overline{\varphi}$ is the mean potential in the WS cell [5]. The prefactors $\rho_0^{\pm}$ are then determined by

$$\rho_0^{\pm} = n^{\pm} \equiv \frac{N_{\pm}}{V} \equiv \frac{1}{V}\int_V \rho^{\pm}(\boldsymbol{r})\ \mathrm{d}^3 r \tag{2}$$

where N_+ (N_-) is the number of counter-ions (co-ions) in the WS cell of volume V. Note that $n_s = n^-$ is the salt concentration and that the electroneutrality constraint reads $N_+ - N_- = Z$.

In the situations considered here, the boundary conditions involve the electric field, so it is possible to impose $\overline{\varphi} = 0$. The approximate densities are then

$$\rho^{\pm}(\boldsymbol{r}) = \rho_0^{\pm}\left[1 \mp \beta e\varphi(\boldsymbol{r})\right] \tag{3}$$

and denoting the charge density of the platelet by $q_{\mathcal{P}}$, the electrostatic potential is determined by Poisson's equation:

$$\nabla^2\varphi(\boldsymbol{r}) = -\frac{4\pi}{\varepsilon} q_{\mathcal{P}}(\boldsymbol{r}) + \kappa_D^2\left[\varphi(\boldsymbol{r}) - \gamma_0\right] \tag{4}$$

where

$$\gamma_0 = \frac{kT}{e}\frac{\rho_0^+ - \rho_0^-}{\rho_0^+ + \rho_0^-} \qquad \text{and} \qquad \kappa_D^2 = 4\pi\frac{\beta e^2}{\varepsilon}(\rho_0^+ + \rho_0^-) = 1/\lambda_D^2. \tag{5}$$

κ_D^2 is the squared inverse Debye length. The strength of electrostatic interactions is characterized by the Bjerrum length $\ell_B = \beta e^2/\varepsilon$.

In the canonical situation, the concentrations $n^\pm$ are known *a priori*, whereas in the case where the system is in equilibrium with a salt reservoir of concentration n_s', the condition of equal salt chemical potentials in the solution and in the reservoir yields $\rho_0^+\rho_0^- = (n_s')^2$. As a consequence, n_s is given by (the Donnan effect)

$$n_s = \sqrt{(n_s')^2 + \frac{Z^2}{4}n^2} - \frac{Z}{2}n. \tag{6}$$

The clay concentration n in the solution fixes the average volume of the WS cell. For a given shape (cylinder or parallelepiped), the free energy F of the double layer must be minimized with respect to the aspect ratio equal to the height over the radius or edge length of the base, the volume of the cell being kept constant. If the system is in osmotic equilibrium with a salt reservoir, the difference between the grand potential Ω to be minimized and F is independent of the aspect ratio of the cell, since

$$\Omega - F = -\mu_{\text{salt}}N_{\text{salt}} = -N_{\text{salt}}kT\log(n_s'\Lambda^3)$$

and so the potential to be minimized is still F. In the following examples, F has been calculated analytically using a constant-Debye-length charging process from a situation where the platelets are neutral ($Z = 0$) to that where $Z = Z^{\text{final}}$ [5]. For uncharged platelets, $N_+^0 = N_-^0 = N^0 = Vn_s + Z/2$. At any stage of the process, $N_\pm = N^0 \pm Z/2$, and in the elementary step $Z \to Z + \delta Z$

$$\delta F = \int_{\mathcal{P}} \varphi\,\delta\sigma\ \mathrm{d}^2r + kT\left[\log(\rho_0^+\Lambda^3)\right]\delta N_+ + kT\left[\log(\rho_0^-\Lambda^3)\right]\delta N_- \tag{7}$$

where σ denotes the surface charge of the platelet ($\sigma = -Ze/S < 0$). The integration along this path gives

$$F - F(Z=0) = A - Ze\gamma_0 + N^0kT\log\left\{\frac{(N^0)^2 - Z^2/4}{(N^0)^2}\right\} + \frac{Z}{2}kT\log\left\{\frac{N^0 + Z/2}{N^0 - Z/2}\right\} \tag{8}$$

where

$$A = \int_0^\sigma \left[\int_{\mathcal{P}} (\varphi_{\mathcal{P}}^{\sigma'} - \gamma_0)\ \mathrm{d}^2r\right]\ \mathrm{d}\sigma'. \tag{9}$$

3. Disc-shaped platelets

3.1. The cylindrical Wigner–Seitz cell

When the WS cell is a cylinder of height $H = 2h$ and radius R, the potential can be expanded in a Bessel–Dini series [9] which is well adapted to the condition of a vanishing normal electric field on the surface Σ [4]. The radius of the platelet is denoted by r_0. Using cylindrical coordinates (r, z), the solution of equation (4) reads [4]

$$\begin{aligned}\beta e\varphi(r,z) = \beta e\gamma_0 &+ \frac{1}{\kappa_D b}\left(\frac{r_0}{R}\right)^2\frac{\cosh[\kappa_D(h-|z|)]}{\sinh(\kappa_D h)} \\ &+ \frac{2}{b}\frac{r_0}{R}\sum_{n=2}^{\infty}\frac{\Lambda_n J_1(k_n r_0)}{y_n\sinh(h/\Lambda_n)J_0^2(y_n)}\cosh\left(\frac{h-|z|}{\Lambda_n}\right)J_0(k_n r)\end{aligned} \tag{10}$$

where y_n is the nth root of $J_1(y) = -\mathrm{d}J_0(y)/\mathrm{d}y = 0$, J_0 and J_1 are the Bessel functions of zeroth and first order ($y_1 = 0$), $\Lambda_n = R/\sqrt{(y_n^2 + \kappa_D^2 R^2)}$, $k_n = y_n/R$, and $b = e/(2\pi \ell_B \sigma) < 0$ is the Gouy length.

The first non-vanishing multipole of the charge distribution is the quadrupole $Q = Q_{zz} = -2Q_{xx} = -2Q_{yy}$ with the (Oz) axis orthogonal to the disc:

$$Q_{zz}^{\mathrm{tot}} = \int_V \left\{ q_{\mathcal{P}}(\boldsymbol{r}) + e\left[\rho^+(\boldsymbol{r}) - \rho^-(\boldsymbol{r})\right]\right\} (2z^2 - x^2 - y^2)\ \mathrm{d}^3 r. \tag{11}$$

For an oblate distribution of negatively charged ions, $Q_{zz} > 0$ (e.g. $Q_{zz}^{\mathrm{disc}} = Zer_0^2/4$). From expression (10) for the potential

$$\frac{Q_{zz}^{\mathrm{tot}}}{Q_{\mathrm{disc}}} = 1 - \frac{8}{\kappa_D^2 r_0^2 \sinh(\kappa_D h)} \left[\kappa_D h + \left(\frac{R^2 \kappa_D^2}{8} - 1 \right) \sinh(\kappa_D h) \right] - \frac{16 R^3 \kappa_D^2}{r_0^3} \sum_{n=2}^{\infty} \frac{\Lambda_n^2 J_1(k_n r_0)}{y_n^3 J_0(y_n)}. \tag{12}$$

The free energy can also be calculated, leading to the following expression for A (cf. equation (8)):

$$\frac{\beta}{Z} A = \frac{1}{2\kappa_D b} \left\{ \left(\frac{r_0}{R} \right)^2 \frac{1}{\tanh(\kappa_D h)} + 4 \sum_{n=2}^{\infty} \frac{\kappa_D \Lambda_n J_1^2(k_n r_0)}{y_n^2 J_0^2(y_n) \tanh(h/\Lambda_n)} \right\}. \tag{13}$$

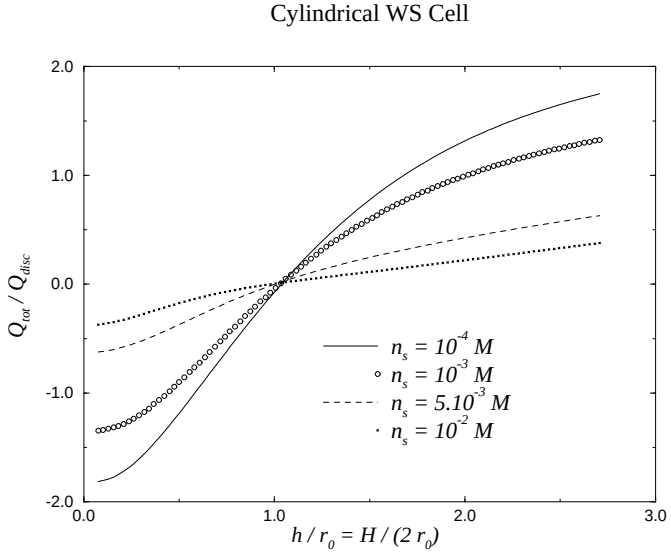

Figure 1. The aspect ratio dependence of the total normalized quadrupole for a clay concentration $n = 5 \times 10^{-5}$ M. The platelets carry $Z = 100$ elementary charges, $\varepsilon_{C.G.S.} = 78$ and $T = 300$ K.

Figure 1 shows the aspect ratio dependence of the quadrupolar moment for different salinities n_s. For a given clay concentration n, only the product $2\pi R^2 h = 1/n$ is fixed. The aspect ratio h/R (or equivalently h/r_0) is determined by minimizing the free energy as shown in figure 2. The value obtained satisfies the physical requirement $R > r_0$.

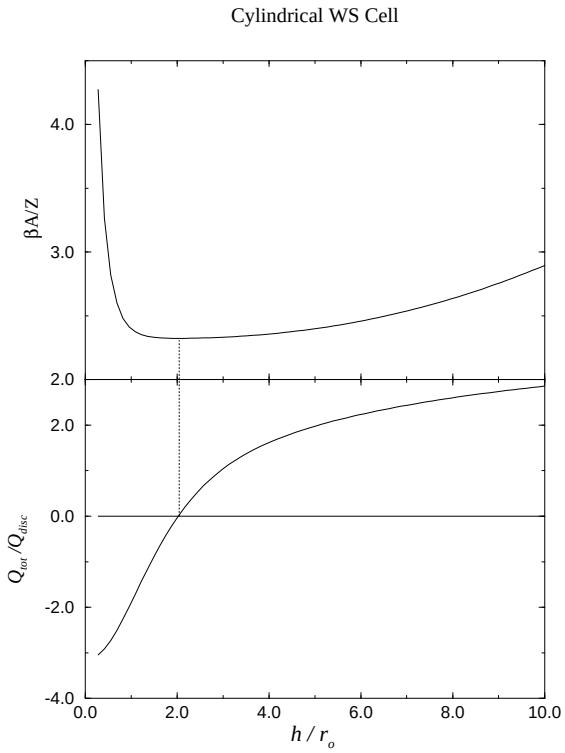

Figure 2. The free energy as a function of the aspect ratio h/r_0, for a constant-volume cell. Here, $n = 10^{-5}$ M, $n_s = 10^{-3}$ M and $Z = 100$. The free energy is a minimum for $2.048 < h/r_0 < 2.055$. For this equilibrium value of the aspect ratio, the total quadrupole vanishes: $Q^{tot} = 0$ between $h/r_0 = 2.024$ and 2.027.

A noteworthy feature of this system is that for this 'optimal' aspect ratio, the ionic distribution around $\mathcal{P}$ corresponds to a vanishing total quadrupole moment (cf. figure 2). Within numerical errors, this coincidence has been observed for all concentrations (n, n_s) investigated. A plausible explanation is proposed in the concluding section.

3.2. The hybrid Poisson–Boltzmann/Debye–Hückel theory

In a Bessel–Dini expansion

$$\varphi(r, z) = \sum_{n=1}^{\infty} A_n(z) J_0\left(y_n \frac{r}{R}\right) \tag{14}$$

the term $n = 1$ ($y_1 = 0$) corresponds to the average potential $\overline{\varphi}^z$ on $z =$ constant planes, as may be concluded from the relation

$$\int_0^R r J_0\left(y_n \frac{r}{R}\right) \mathrm{d}r = \frac{R^2}{y_n} J_1(y_n) = 0. \tag{15}$$

Notice also that the term $n = 1$ in expansion (10) corresponds to the solution of equation (4) in the case of an infinite plane in a WS slab of height $2h$, with an effective surface

charge $\sigma' = \sigma r_0^2/R^2$:

$$\varphi(r,z) = \gamma_0 + \frac{2kT}{e\kappa_D b}\frac{\cosh[\kappa_D(h-|z|)]}{\sinh(\kappa_D h)}. \tag{16}$$

The Gouy length b is associated with the effective charge σ', i.e.: $b = e/(\pi\ell_B\sigma')$. The summation $n \geqslant 2$ can therefore be considered as a finite-size correction to the $r_0 \to \infty$ limit of the fully linearized Poisson–Boltzmann theory. We may expect to obtain an estimate of this r-dependent correction to the non-linear one-dimensional Gouy–Chapman theory by keeping the non-linear term $n = 1$ in the density profiles and by linearizing the potential around $\overline{\varphi}^z = A_1(z)$:

$$\rho^{\pm}(\boldsymbol{r}) = \rho_0^{\pm}\exp\left[\mp\beta e A_1(z)\right]\left\{1 \mp \beta e\sum_{n=2}^{\infty} A_n(z)J_0\left(y_n\frac{r}{R}\right)\right\}. \tag{17}$$

As a consequence,

$$n^{\pm} = \rho_0^{\pm}\frac{1}{2h}\int_{-h}^{h}\exp\left[\mp\beta e A_1(z)\right]\,\mathrm{d}z \tag{18}$$

and it is *a priori* impossible to impose $\rho_0^+ = n^+$ and $\rho_0^- = n^-$ simultaneously.

For $z \neq 0$, the semi-linearized PB equation reads

$$\nabla^2\varphi(\boldsymbol{r}) = -\frac{4\pi e}{\varepsilon}\left[\rho_0^+\exp(-\beta e A_1) - \rho_0^-\exp(\beta e A_1)\right] + 4\pi\ell_B\left[\rho_0^+\exp(-\beta e A_1) + \rho_0^-\exp(\beta e A_1)\right]\left\{\sum_{n=2}^{\infty} A_n(z)J_0\left(y_n\frac{r}{R}\right)\right\}. \tag{19}$$

The boundary condition associated with the presence of the uniformly charged platelet located at $z = 0$, $r < r_0$ is

$$\left.\frac{\mathrm{d}\varphi}{\mathrm{d}z}\right|_{z=0^+} = -\frac{2\pi\sigma}{\varepsilon}\Theta(r_0 - r) \tag{20}$$

where Θ is the Heaviside function. On top of the cylinder ($z = \pm h$), the electric field vanishes, i.e. $\mathrm{d}\varphi/\mathrm{d}z = 0$.

Projection on the basis functions J_0 leads to the differential equations

$$\frac{\mathrm{d}^2A_1(z)}{\mathrm{d}z^2} = -\frac{4\pi e}{\varepsilon}\left[\rho_0^+\exp(-\beta e A_1) - \rho_0^-\exp(\beta e A_1)\right] \tag{21a}$$

$$\frac{\mathrm{d}^2A_n(z)}{\mathrm{d}z^2} - \left(\frac{y_n}{R}\right)^2 A_n(z) = 4\pi\ell_B\left[\rho_0^+\exp(-\beta e A_1) + \rho_0^-\exp(\beta e A_1)\right]A_n(z) \qquad n \geqslant 2. \tag{21b}$$

The Heaviside step function can be expanded in a Bessel–Dini series:

$$\Theta(r_0 - r) = \left(\frac{r_0}{R}\right)^2 + \frac{2r_0}{R}\sum_{n=2}^{\infty}\frac{1}{y_n J_0^2(y_n)}J_1\left(\frac{y_n r_0}{R}\right)J_0\left(\frac{y_n r}{R}\right) \tag{22}$$

so the boundary condition for $z \to 0$ translates into

$$\frac{\mathrm{d}A_1(z)}{\mathrm{d}z} = -\frac{2\pi\sigma}{\varepsilon}\left(\frac{r_0}{R}\right)^2 \tag{23a}$$

$$\frac{\mathrm{d}A_n(z)}{\mathrm{d}z} = -\frac{4\pi\sigma r_0}{\varepsilon R}\frac{1}{y_n J_0^2(y_n)}J_1\left(\frac{y_n r_0}{R}\right) \qquad n \geqslant 2 \tag{23b}$$

and

$$\left.\frac{\mathrm{d}A_n(z)}{\mathrm{d}z}\right|_{z=\pm h} = 0 \qquad n \geqslant 1. \tag{24}$$

As expected, the term $A_1(z)$ is the solution of the corresponding one-dimensional non-linear Gouy–Chapman problem (the infinite disc), with an effective surface charge $\sigma' = \sigma r_0^2/R^2$. Once this solution is known, it must be injected into equations (21*b*) which are linear in the A_n; the resulting equations generally turn out to be analytically intractable and require a numerical integration. In the appendix, we will present the simplest example, for which a fully analytical solution can be obtained.

3.3. Parallelepipedic Wigner–Seitz cells

If the WS cell is a parallelepiped of dimensions $L \times L \times H$ in the x-, y- and z-directions respectively, the potential can be expanded in plane waves compatible with the periodic boundary conditions. These are equivalent to the condition of a vanishing normal component of the electric field on Σ:

$$\varphi(\boldsymbol{r}) = \sum_{\boldsymbol{k}} \widetilde{\varphi}(\boldsymbol{k}) \exp\{\mathrm{i}\boldsymbol{k}\cdot\boldsymbol{r}\} \tag{25}$$

with

$$\boldsymbol{k} = 2\pi \begin{cases} n_x/L \\ n_y/L \\ n_z/H \end{cases} \qquad (n_x, n_y, n_z) \in \mathbb{Z}^3. \tag{26}$$

In terms of Fourier components, equation (4) becomes

$$(k^2 + \kappa_D^2)(\widetilde{\varphi}(\boldsymbol{k}) - \gamma_0) = \frac{4\pi}{\varepsilon}\widetilde{q}_{\mathcal{P}}(\boldsymbol{k}) \tag{27}$$

where

$$\widetilde{q}_{\mathcal{P}}(\boldsymbol{k}) = \frac{1}{V}\int_V q_{\mathcal{P}}(\boldsymbol{r}) \exp\{\mathrm{i}\boldsymbol{k}\cdot\boldsymbol{r}\}\ \mathrm{d}^3r. \tag{28}$$

A little algebra yields

$$\widetilde{q}_{\mathcal{P}}(\boldsymbol{k}) = \frac{2\pi r_0}{k_\parallel}\frac{\sigma}{V} J_1(k_\parallel r_0) \qquad \text{with } k_\parallel = \frac{2\pi}{L}\sqrt{n_x^2 + n_y^2}. \tag{29}$$

Hence, the expression of the electrostatic potential is

$$\beta e\varphi(\boldsymbol{r}) = \beta e\gamma_0 + \frac{4\pi}{b}\frac{r_0}{L^2 H}\sum_{(n_x,n_y,n_z)\in\mathbb{Z}^3} \frac{J_1(k_\parallel r_0)}{k_\parallel(k^2+\kappa_D^2)}\cos(\boldsymbol{k}\cdot\boldsymbol{r}). \tag{30}$$

For the corresponding quadrupolar moment, one finds

$$\frac{Q_{zz}^{\mathrm{tot}}}{Q_{\mathrm{disc}}} = -\frac{16}{r_0^3}\left\{\sum_{n_z=1}^{\infty}\frac{(-1)^{n_z}}{k_z^2+\kappa_D^2}r_0 - \sum_{n_x=1}^{\infty}\frac{J_1(k_x r_0)}{k_x^2+\kappa_D^2}(-1)^{n_x}\frac{2}{k_x}\right\} \tag{31}$$

and the same procedure as above yields the free energy:

$$\frac{\beta}{Z}A = -\frac{4\pi}{L^2 H b}\sum_{(n_x,n_y,n_z)\in\mathbb{Z}^3}\frac{J_1^2(k_\parallel r_0)}{k_\parallel^2(k^2+\kappa_D^2)}. \tag{32}$$

It is instructive to estimate the changes in F and Q induced by the change of the topology of the WS cell, compared to the cylindrical case. Figure 3 shows that in spite of the completely different analytical expressions (12)/(31) and (13)/(32), the numerical evaluations yield extremely close results for the given concentrations and aspect ratios. In particular, the minimum of the free energy still coincides with the vanishing of Q_{zz}^{tot}.

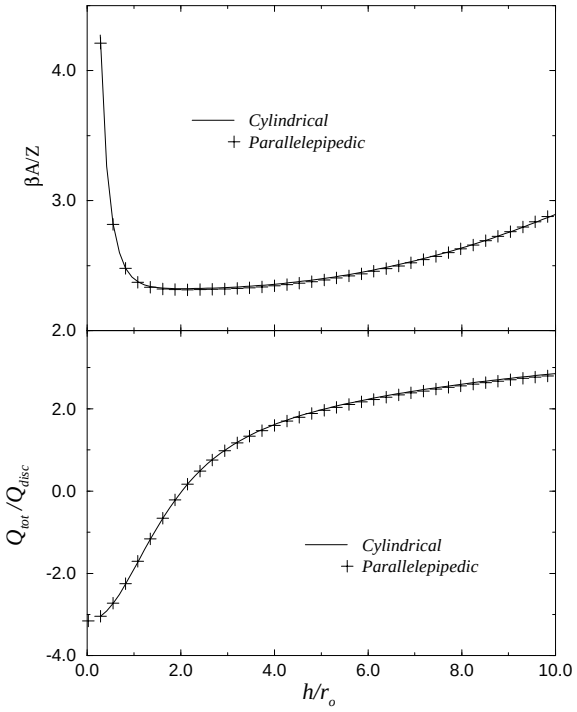

Figure 3. A comparison between the cylindrical and parallelepipedic geometries ($n_s = 10^{-3}$ M, $n = 10^{-5}$ M, $Z = 100$; see figure 2). The whole range of aspect ratios displayed satisfies the physical requirement $r_0 < R$ (cylindrical geometry) or $r_0 < L/2$ (parallelepipedic cell). For these parameters, a cubic cell ($H = L$) corresponds to $H/(2r_0) \simeq 2.2$.

4. Square platelets

The problem of a square platelet of edge length l_0 placed at the centre of a parallelepipedic cell is very similar to the case studied in section 3.3. The potential is once more expanded in plane waves, leading to the form

$$\beta e\varphi(\boldsymbol{r}) = \beta e\gamma_0 + \frac{8}{bL^2H} \sum_{(n_x,n_y,n_z)\in\mathbb{Z}^3} \sin(k_x l_0/2)\sin(k_y l_0/2)\frac{1}{k_x k_y}\frac{1}{k^2+\kappa_D^2}\cos(\boldsymbol{k}\cdot\boldsymbol{r}). \quad (33)$$

The corresponding expression of the total quadrupole is

$$\frac{Q_{zz}^{\mathrm{tot}}}{Q_{\mathrm{platelet}}} = -\frac{48}{l_0^3}\left\{\sum_{n_z=1}^{\infty}(-1)^{n_z}\frac{l_0}{k_z^2+\kappa_D^2} - 2\sum_{n_x=1}^{\infty}(-1)^{n_x}\frac{\sin(k_x l_0/2)}{k_x(k_x^2+\kappa_D^2)}\right\} \quad (34)$$

while for the free energy

$$\frac{\beta}{Z}A = -\frac{16}{l_0^2L^2Hb}\sum_{(n_x,n_y,n_z)\in\mathbb{Z}^3}\frac{\sin^2(k_x l_0/2)\sin^2(k_y l_0/2)}{k_x^2k_y^2(k^2+\kappa_D^2)}. \quad (35)$$

5. Discussion

The main findings of the present work may be summarized as follows.

(a) Over a broad range of physical conditions, the free energy of the distribution of co- and counter-ions within a WS cell goes through a minimum at a physical value of the aspect ratio. This indicates that within the mean-field-like WS description, a particular spacing between platelets in a parallel stacking is selected, under the action of electrostatic forces alone. Obviously the WS picture restricts the possible topologies to columnar stackings, and much more complicated structures should be expected, particularly at low clay concentrations.

(b) In the case of disc-like platelets, the free energy and the quadrupole moment of the charge distribution in the WS cell are practically identical for cylindrical and parallelepipedic cells of equal volume. It seems reasonable to expect that a regular columnar stacking of circular platelets would be of hexagonal symmetry, with a unit cell which is somewhat intermediate in shape between cylindrical and parallelepipedic cells.

(c) For any given clay and salt concentrations, the quadrupole moment of the cell is found to vanish at the aspect ratio which minimizes the free energy. This somewhat surprising finding may be rationalized in the light of the perfect screening properties of Coulombic systems (see e.g. [12]). It can be proven rigorously under rather weak clustering assumptions that the multipole moments of a distribution of charges vanish in states of thermodynamic equilibrium. Hence we expect the total quadrupole moment of a macroscopic suspension of clay platelets to be zero. This property should hold, in particular, if the equilibrium state is a regular columnar stacking of platelets. The quadrupole moment of the unit cell of such a regular array must then also vanish. It may next be argued that, as long as the shape of the WS cells considered in this paper is close to that of the unit cell (expected to be of hexagonal symmetry) of the regular array, the quadrupole moment of the cylindrical or parallelepipedic cells should be close to zero.

(d) We propose a preliminary formulation of a hybrid Poisson–Boltzmann/Debye–Hückel theory to avoid, at least partially, the shortcomings of the linearization of the Boltzmann factors, which becomes very dubious for highly charged platelets. A numerical implementation of this scheme, which correctly incorporates the Gouy–Chapman limit for infinite platelets, will be the subject of a future publication.

Appendix

Let us consider the case of a disc placed at the centre of an infinite cylinder ($h \to \infty$, R finite) without added salt. For this suspension of vanishing clay concentration, the electrostatic potential satisfies, within the hybrid Poisson–Boltzmann/Debye–Hückel formulation presented in section 3.2,

$$\frac{\mathrm{d}^2 A_1(z)}{\mathrm{d}z^2} = -\frac{4\pi e}{\varepsilon}\rho_0^+ \exp(-\beta e A_1) \tag{A1a}$$

$$\frac{\mathrm{d}^2 A_n(z)}{\mathrm{d}z^2} - \left(\frac{y_n}{R}\right)^2 A_n(z) = 4\pi \ell_B \rho_0^+ \exp(-\beta e A_1) A_n(z) \qquad n \geqslant 2. \tag{A1b}$$

For $z \to \infty$, the only physical requirement is $\rho^+(r, z) \to 0$. The Gouy–Chapman solution for $n = 1$ is well known [11]:

$$A_1(z) = \frac{2kT}{e}\log(|z| - b) + A_1^0 \qquad b = \frac{e}{\pi \ell_B \sigma'} < 0 \tag{A2}$$

where $-b$ is the effective Gouy length characterizing the thickness of the double layer for an infinite platelet. Here, the electroneutrality constraint relates the unphysical quantities A_1^0 and ρ_0^+ through $\rho_0^+ \exp(-\beta e A_1^0) = 1/(2\pi \ell_B)$.

For $z > 0$, the higher-order terms ($n \geqslant 2$) in the expansion (14) therefore obey the differential equation

$$\frac{\mathrm{d}^2 A_n(z)}{\mathrm{d}z^2} - \left(\frac{y_n}{R}\right)^2 A_n(z) = \frac{2}{(z-b)^2} A_n(z). \tag{A3}$$

According to equation (17), the condition $\rho^+ \to 0$ for $z \to \infty$ imposes $A_n(z)/z^2 \to 0$. Let us transform (A3) into a canonical form by defining

$$B_n(v) = \frac{4y_n^2}{R^2} A_n(z) \qquad \text{with } v = \frac{2y_n}{R}(z-b). \tag{A4}$$

We obtain

$$\frac{\mathrm{d}^2 B_n}{\mathrm{d}v^2} - \left(\frac{1}{4} + \frac{2}{v^2}\right) B_n = 0 \tag{A5}$$

the solutions of which are Whittaker functions (see for example reference [10], ch XVI):

$$B_n(v) = \alpha_n W_{0,3/2}(v) + \beta_n W_{0,3/2}(-v). \tag{A6}$$

From the asymptotic large-v expansion $W_{0,3/2}(v) \sim \exp(-v/2)$, it follows that $\beta_n = 0$. Finally, using the notation $W' = \mathrm{d}W/\mathrm{d}v$, the boundary condition for $z = 0^+$ translates into

$$\alpha_n = -\frac{1}{W'_{0,3/2}(v = -2y_n b/R)} \frac{8\pi\sigma r_0}{\varepsilon R^2} \frac{1}{J_0^2(y_n)} J_1\left(\frac{y_n r_0}{R}\right) \tag{A7}$$

and the potential takes the form

$$\varphi(r,z) = A_1^0 + \frac{2kT}{e}\log(|z|-b) + \sum_{n=2}^{\infty} \frac{R^2}{4y_n^2}\alpha_n W_{0,3/2}\left\{\frac{2y_n}{R}(|z|-b)\right\} J_0\left(\frac{y_n r}{R}\right). \tag{A8}$$

The corresponding counter-ion profile is

$$\rho^+(\boldsymbol{r}) = \frac{1}{2\pi\ell_B}\frac{1}{(|z|-b)^2}\left\{1 - \frac{\beta e R^2}{4}\sum_{n=2}^{\infty}\frac{1}{y_n^2}\alpha_n W_{0,3/2}\left[\frac{2y_n}{R}(|z|-b)\right] J_0\left(\frac{y_n r}{R}\right)\right\}. \tag{A9}$$

References

[1] van Olphen H 1977 *Clay Colloid Chemistry* 2nd edn (New York: Wiley)
[2] *Laporte Inorganics Laponite Technical Bulletin* L104/90/A
[3] For a simplified model, see recent simulation work by
Dijkstra M, Hansen J-P and Madden P A 1995 *Phys. Rev. Lett.* **75** 2236
[4] Hansen J-P and Trizac E 1997 *Physica* A at press
[5] Trizac E and Hansen J-P 1996 *J. Phys.: Condens. Matter* **8** 9191
[6] See, e.g.,
Barker J A 1963 *Lattice Theory of the Liquid State* (New York: MacMillan)
[7] See, e.g.,
Groot J D 1991 *J. Chem. Phys.* **95** 9191
[8] Fuoss R M, Katchalsky A and Lifson S 1951 *Proc. Natl Acad. Sci., USA* **37** 579
[9] Watson G N 1958 *A Treatise on the Theory of Bessel Functions* 2nd edn (Cambridge: Cambridge University Press)
[10] Whittaker E T and Watson G N 1965 *A Course of Modern Analysis* 4th edn (Cambridge: Cambridge University Press)
[11] For a recent review, see
Andelman D 1995 *Sructure and Dynamics of Membranes* ed R Lipowsky and E Sackmann (Amsterdam: Elsevier)
[12] Martin P A 1988 *Rev. Mod. Phys.* **60** 1075